J. Phys. Chem. A **2006,** *110,* 6433−6438

Investigation of the Two-Photon Absorption Cross-Section in Perylene Tetracarboxylic Derivatives: Nonlinear Spectra and Molecular Structure

Daniel S. Corrêa,[†] Samuel L. Oliveira,[†,‡] Lino Misoguti,[†] Sérgio C. Zilio,[†] Ricardo F. Aroca,[§] Carlos J. L. Constantino,[⊥] and Cleber R. Mendonça*,[†,||]

Instituto de Física de São Carlos, Universidade de São Paulo, CP 369, 13560-970, São Carlos, SP, Brazil, Departamento de Física, Química e Biologia, UNESP, CP 467, 19060-900, Presidente Prudente, SP, Brazil, and Materials and Surface Science Group, University of Windsor, Windsor, ON, N9B 3P4, Canada

Received: December 5, 2005; In Final Form: March 21, 2006

We investigated the 2PA absorption spectrum of a family of perylene tetracarboxylic derivatives (PTCDs): bis(benzimidazo)perylene (AzoPTCD), bis(benzimidazo)thioperylene (Monothio BZP), *n*-pentylimidobenzimidazoperylene (PazoPTCD), and bis(*n*-butylimido)perylene (BuPTCD). These compounds present extremely high two-photon absorption, which makes them attractive for applications in photonics devices. The two-photon absorption cross-section spectra of perylene derivatives obtained via *Z*-scan technique were fitted by means of a sum-over-states (SOS) model, which described with accuracy the different regions of the 2PA cross-section spectra. Frontier molecular orbital calculations show that all molecules present similar features, indicating that nonlinear optical properties in PTCDs are mainly determined by the central portion of the molecule, with minimal effect from the lateral side groups. In general, our results pointed out that the differences in the 2PA cross-sections among the compounds are mainly due to the nonlinearity resonance enhancement.

Introduction

The first investigations involving perylene compounds as potential materials for applications in electronics and optics were carried out by Graser and co-workers.[1−3] Their studies were dedicated to the development of fluorescent perylene derivatives and the study of their crystalline structure. However, in the past decade perylene compounds were tested in many other technological applications such as Langmuir−Blodgett films,[4] laser action,[5] and also solar cells.[6] Recently, we have reported two perylene derivatives with extremely large two-photon absorption cross-sections,[7] which could be candidates for applications in upconversion lasing and optical limiting. Molecules undergo two-photon absorption (2PA) when exposed to high-intensity light sources, reaching a final state by the simultaneous absorption of two photons, each one with half of the energy required for the electronic transition.

One of the advantages related to this process is its quadratic dependence with the irradiance that makes possible to confine the laser excitation in a minute spatial volume. In addition, 2PA processes allow higher depth penetration and lower scattering losses due to the insignificant absorption outside the focal volume, and the employment of low-energy photons. Such features have led to a large number of technological applications, such as lithographic microfabrication,[8,9] three-dimensional optical data storage,[10,11] fluorescence excitation microscopy, two-photon photodynamic therapy,[12,13] and two-photon pumped lasing.[14]

In the last years there has been a great effort to synthesize new materials that present extremely large 2PA cross-sections, thus leading to a decrease in the excitation irradiance, allowing the use of less expensive and simpler laser systems as well as attenuating the drawback related to the compound damage threshold. Within this context, we have reported recently[7] perylene tetracarboxylic derivatives (PTCDs) compounds as promising materials for 2PA applications in optical limiting and upconversion lasing thanks to extremely large 2PA cross-sections. In this work, the results of a complete study on the degenerate 2PA spectra of four PTCD compounds, (benzimidazo)perylene (AzoPTCD), bis(benzimidazo)thioperylene (Monothio BZP), pentylimidobenzimidazoperylene (PazoPTCD), and bis(*n*-butylimido)perylene (BuPTCD) are presented. The features observed in the 2PA spectrum, resonance enhancement of the nonlinearity and 2PA peak, could be fitted with a sum-over-states model (SOS),[15,16] allowing a better comprehension of the observed results. As an attempt to further understand the large nonlinear optical property (2PA) of the perylene derivatives and relate it to the molecular structures, molecular orbital calculations with semi-empirical methods were carried out.

Experimental and Computational Details

1. Compounds. AzoPTCD, Monothio BZP, PazoPTCD, and BuPTCD compounds were obtained from Xerox Research Centre of Canada (XRCC). The powders were dissolved in 10% by volume trifluoroacetic acid (TFA)/dichloromethane and placed in a 2-mm-thick quartz cuvette for the spectroscopic measurements.

2. Optical Measurements. The linear and nonlinear optical measurements of the PTCD compounds were obtained with concentrations on the order of 10^{-5} and 10^{-3} mol L^{-1},

---

* To whom correspondence should be addressed. E-mail: crmendon@if.sc.usp.br.

[†] Universidade de São Paulo.

[‡] Present address: Optical Science Laboratory, Department of Electrical Engineering and Computer Science, University of Michigan, Ann Arbor, Michigan, 48109-2122.

[§] University of Windsor.

[⊥] UNESP.

[||] Present address: Division of Engineering and Applied Sciences and Department of Physics, Harvard University, 9 Oxford Street, Cambridge, MA 02138.

10.1021/jp057065e CCC: $33.50

respectively. The linear absorption spectra were recorded on a Cary 50 spectrophotometer. The 2PA absorption spectra were obtained by using the *Z*-scan technique (for further details also see refs 17 and 18). The latter technique is used to determine the 2PA β coefficient with considerable accuracy by moving the sample through the focal plane of a focused Gaussian beam and monitoring the corresponding changes in the far field intensity. In the case of nonlinear absorption, the light field creates an intensity dependence given by, $\alpha = \alpha_0 + \beta I$, where I is the laser beam irradiance and α_0 is the linear absorption coefficient. The β coefficient can then be determined by monitoring the change in transmittance as the sample is scanned through the focal position. In off-resonant conditions, such as in 2PA, the change in the transmitted power is integrated over time to give the normalized energy transmittance, and assuming a temporally Gaussian pulse,[18]

$$T = \frac{1}{\sqrt{\pi}q_0(z,0)}\int_{-\infty}^{\infty} \ln[1 + q_0(z,0)e^{-\tau^2}]\, d\tau \qquad (1)$$

where $q_0(z,t) = \beta I_0(t)L(1 + z^2/z_0^2)^{-1}$, L is the sample thickness, z_0 is the Rayleigh length, z is the sample position, and I_0 is the pulse irradiance. The nonlinear coefficient β is obtained by fitting the *Z*-scan signatures with use of eq 1.[18] The 2PA cross-section, δ, is determined through the expression $\delta = h\nu\beta/N$, where $h\nu$ is the excitation photon energy and N is the number of molecules per cm^3. Usually, the unit used to express δ is the Göppert−Mayer (GM), in which 1 GM = 1 × 10^{-50} cm^4 s molecules^{-1} photon^{-1}. In our *Z*-scan experiment we employed laser pulses with 120 fs from 1100 to 590 nm using an optical parametric amplifier (TOPAS, from Light Conversion) pumped by 150 fs pulses at 775 nm delivered by a commercial Ti:sapphire chirped pulse amplified system (CPA-2001 from Clark-MXR Inc.), which operates at 1 kHz repetition rate. A Gaussian distribution of the beam profile was achieved by using appropriate spatial filtering. The output signal was monitored with a silicon PIN photodetector coupled to a lock-in amplifier.

3. Computational Details. The AM1 semi-empirical method[19] from Hyperchem 5.0 was employed to optimize the geometry of all PTCDs. From the optimized geometry of the molecules, the orbital molecular calculations were performed with use of ZINDO/S method.[20]

Results and Discussion

The vibronic structure of the visible electronic absorption band spanning the 440−680 nm spectral regions is characteristic of all PTCDs and is shown in Figure 1. However, these compounds are completely transparent in the near-infrared region above 700 nm.

As mentioned before, the 2PA spectra of the PTCD materials were determined by using the *Z*-scan technique[17,18] with femtosecond laser pulses. Figure 2 shows a typical *Z*-scan for AzoPTCD and Monothio BZP compounds, using an off-resonance pump wavelength at 770 nm. The solid line represents the fitting of the experimental data obtained with eq 1. The inset in Figure 2 displays the transmittance change as a function of the pump irradiance taken from the *Z*-scan curves of the PTCDs. The linear behavior presented is typical for a 2PA process.[18]

Performing *Z*-scan measurements at different wavelengths followed by fitting the experimental results with eq 1, it is possible to determine the 2PA cross-sections of the PTCDs within a large spectral range. The experimental results taken from the fitted curves are shown in Figure 3.

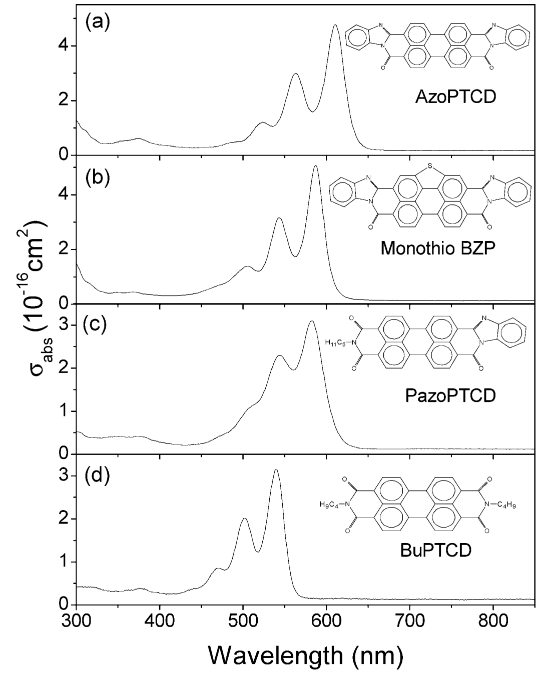

Figure 1. Linear absorption cross section of AzoPTCD, MonothioBZP, PazoPTCD, and BuPTCD. The insets show the respective molecular structure.

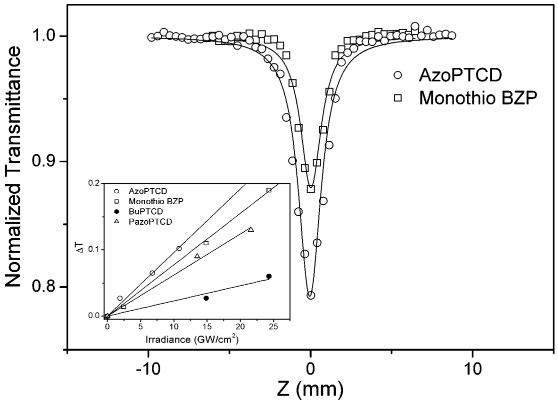

Figure 2. *Z*-scan signatures for AzoPTCD and Monothio BZP in a solution of 10% by volume (TFA)/dichloromethane (approximately 2 × 10^{-3} mol/L), performed with an intensity of about 20 GW cm^{-2}. The solid lines represent the fitting of the experimental data with eq 1. The inset shows the linear behavior of the transmittance change as a function of the pump irradiance for the PTCD derivatives.

The PTCDs exhibit strong 2PA cross sections at several excitation wavelengths. For instance, AzoPTCD displays an enormous 2PA cross-section, reaching a peak value of 8500 GM (1 GM = 10^{-50} cm^4 s molecule^{-1} photon^{-1}), which is one the largest reported values for organic materials. A remarkable feature observed in all 2PA spectra is the monotonic increase of the 2PA cross-section in the spectral region close to the onset of the linear absorption. This unique behavior can be attributed to the resonant enhancement of the nonlinearity as predicted by the increase of the denominator in the sum-over-states model, when the excitation wavelength approaches the linear absorption band.[15,16,21] The shoulder observed in the nonlinear spectra in the region of the resonant enhancement (monotonic increase) was identified as a 2PA state, and could also be fitted by using the SOS model.[15,16,21] In this analysis we have adopted a four-level energy diagram to explain our results, which is displayed in the inset of Figure 3a. The SOS model, in this approximation,

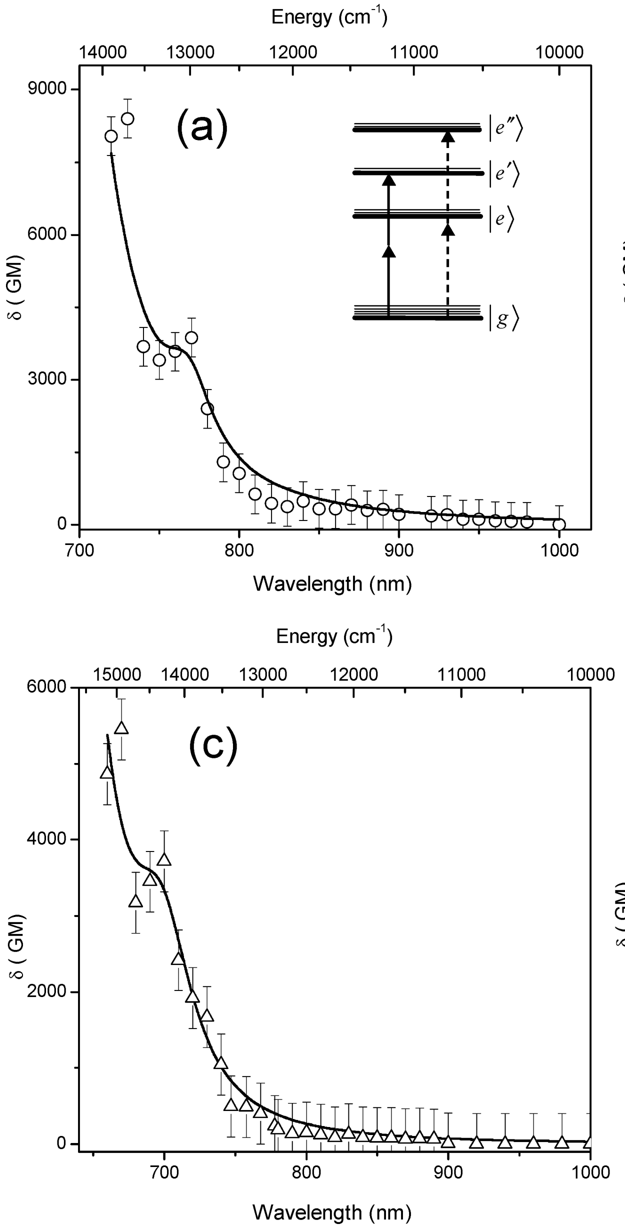

Figure 3. Two-photon absorption cross-section spectra of (a) AzoPTCD, (b) Monothio BZP, (c) PazoPTCD, and (d) BuPTCD in a solution of 10% by volume TFA. The solid lines represent the theoretical fitting obtained with the SOS model taking into account the four-level energy diagram shown in the inset of part a.

predicts a 2PA cross-section $\delta(\nu)$ dependence on the excitation laser frequency, ν, according to

$$\delta(\nu) \propto \frac{\nu^2}{(\nu_{eg} - \nu)^2 + \Gamma_{eg}{}^2}\left[\frac{A_1}{(\nu_{e'g} - 2\nu)^2 + \Gamma_{e'g}{}^2} + \frac{A_2}{(\nu_{e''g} - 2\nu)^2 + \Gamma_{e''g}{}^2}\right] \quad (2)$$

where ν_{mn} and Γ_{mn} represents, respectively, the transition energy and damping constant of the $n \rightarrow m$ transition. In this equation, $A_1 = |\mu_{e'e}|^2|\mu_{eg}|^2\Gamma_{e'g}$ and $A_2 = |\mu_{e''e}|^2|\mu_{eg}|^2\Gamma_{e''g}$.

According to eq 2, the 2PA cross-section is determined by the 2PA line shape functions (terms inside the brackets) for two-photon transitions to the bands $|e'\rangle$ (solid arrow in the inset of Figure 3) and $|e''\rangle$ (dashed arrow in the inset of Figure 3). As the laser frequency approaches the one-photon transition (intermediate state $|e\rangle$), the 2PA tensor term, outside the brackets, increases its contribution resulting in the one-photon resonance enhancement. The terms A1 and A2 in eq 2, which contain the transition dipole moments, were kept floating in the fitting, and the results pointed out similar values for all compounds.

The solid lines in Figure 3a,b,c,d represent the theoretical fitting for AzoPTCD, Monothio BZP, PazoPTCD, and BuPTCD, respectively, which were obtained by using eq 2 with $\nu_{e'g}$, Γ_{eg}, and $\Gamma_{e'g}$ set as fixed parameters, taken from the linear and nonlinear absorption spectra. The $\nu_{e''g}$ and $\Gamma_{e''g}$, which are parameters for the energy and damping factor for the $|e''\rangle$ level, respectively, were allowed to float and be determined by fitting the experimental data. All parameters are shown in Table 1. As the linear absorption spectrum of PTCDs presents a vibronic structure, we have chosen ν_{eg} as an average value, weighted over the vibronic fine structure.

The $|g\rangle \rightarrow |e'\rangle$ transition observed in the 2PA spectra (shoulder) is dark in the linear absorption spectra of PTCD

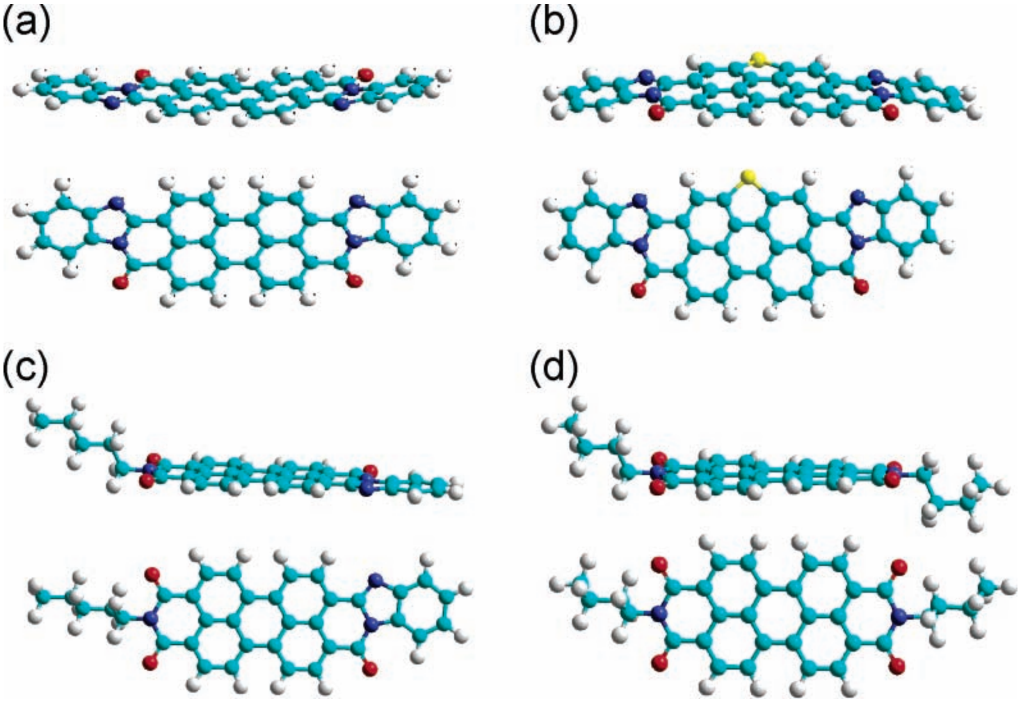

Figure 4. Optimized geometries of AzoPTCD (a), Monothio BZP (b), PazoPTCD (c), and BuPTCB (d) with the AM1 method.

TABLE 1: Spectroscopic Parameters Used in the SOS Model

samples	ν_{eg} (cm^{-1})	$\nu_{e'g}$ (cm^{-1})	$\nu_{e''g}$ (cm^{-1})	Γ_{eg} (cm^{-1})	$\Gamma_{e'g}$ (cm^{-1})	$\Gamma_{e''g}$(cm^{-1})
AzoPTCD	17241 (580 nm)	26316 (380 nm)	30303 (330 nm)	4500	600	1100
Monothio BZP	18868 (530 nm)	26316 (380 nm)	29412 (340 nm)	5000	850	1200
PazoPTCD	18868 (530 nm)	28571 (350 nm)	32051 (312 nm)	5000	1100	1300
BuPTCD	20833 (480 nm)	28571 (350 nm)	34014 (294 nm)	4800	1100	1600

molecules due to symmetry and the corresponding selection rules of dipole transitions. A close examination of Figure 3 reveals that the region of monotonic increase of 2PA bears the same characteristics for all perylene derivatives, except by the position of the 2PA state ($|e'\rangle$), indicating that the lateral side groups of the PTCD molecules have a negligible influence on the resonance enhancement. It can be said that the steepness of the enhancement is mainly determined by the chromophore group in the molecule.

There is extensive literature compiling materials that present large 2PA, but only in the last years have some studies tried to establish a relationship between 2PA properties and molecular structure, including molecular orbital calculations.[22-24] In this work, frontier molecular orbital calculations were performed to assist in the interpretation of the high 2PA cross-sections of the PTCD materials and in an effort to establish a connection with their molecular structures and charge distributions. It is important to emphasize that although the molecular geometries and frontier orbitals were calculated by semi-empirical methods, they suffice to discuss the trends observed in the 2PA spectra of the molecules investigated. Therefore, the molecular orbital results presented here were used only to provide qualitative information on the nonlinearity−molecular structure relationship.

The optimized geometries of the PTCDs by the AM1 method are displayed in Figure 4 over different perspectives. AzoPTCD (a) and Monothio BZP (b) are almost planar probably due to their lateral side groups (benzene rings), which are symmetrically distributed in the molecules. Conversely, PazoPTCD (c) has an alkyl lateral side group forcing a nonplanarity in the entire molecule. BuPTCD (d) also presents a nonplanar molecular structure due to its two alkyl lateral side groups that provide a trans configuration. Nonetheless, all the PTCDs have a central planar chromophore, a determining characteristic of nonlinear optical molecules.

TABLE 2: Computed HOMO and LUMO Energies of the Ground State and Excited State of AzoPTCD, Monothio BZP, PazoPTCD, and BuPTCD

	AzoPTCD	Monothio BZP	PazoPTCD	BuPTCD
HOMO-1 (eV)	−7.95	−7.95	−8.20	−9.49
HOMO (eV)	−7.37	−7.32	−7.54	−7.82
LUMO (eV)	−2.27	−2.29	−2.28	−2.30
LUMO+1 (eV)	−0.97	−0.97	−0.94	−0.92

With use of the ZINDO/S semi-empirical method[20] the frontier molecular orbitals of the PTCD compounds with optimized geometries were calculated. The values of the HOMO-1, HOMO, LUMO, and LUMO+1 are displayed in Table 2.

The energies of HOMO-1, HOMO, LUMO, and LUMO+1 of AzoPTCD and Monothio BZP are quite close, showing that the attachment of a sulfur atom does not cause a significant change in the charge distribution. This feature can also be observed in the representation of the frontier orbitals of AzoPTCD and Monothio BZP in Figure 5.

The planar conjugated aromatic chromophore, a determining factor in the enhanced nonlinear optical properties, presents charge localization as can be seen in Figure 5. The presence of donor groups in AzoPTCD, Monothio BZP, and PazoPTCD further enhances the conjugation length. The latter does not hold for BuPTCD as can be seen in the HOMO and LUMO representation. Therefore, it seems reasonable to assume that the nonlinear optical properties in the PTCD family studied here

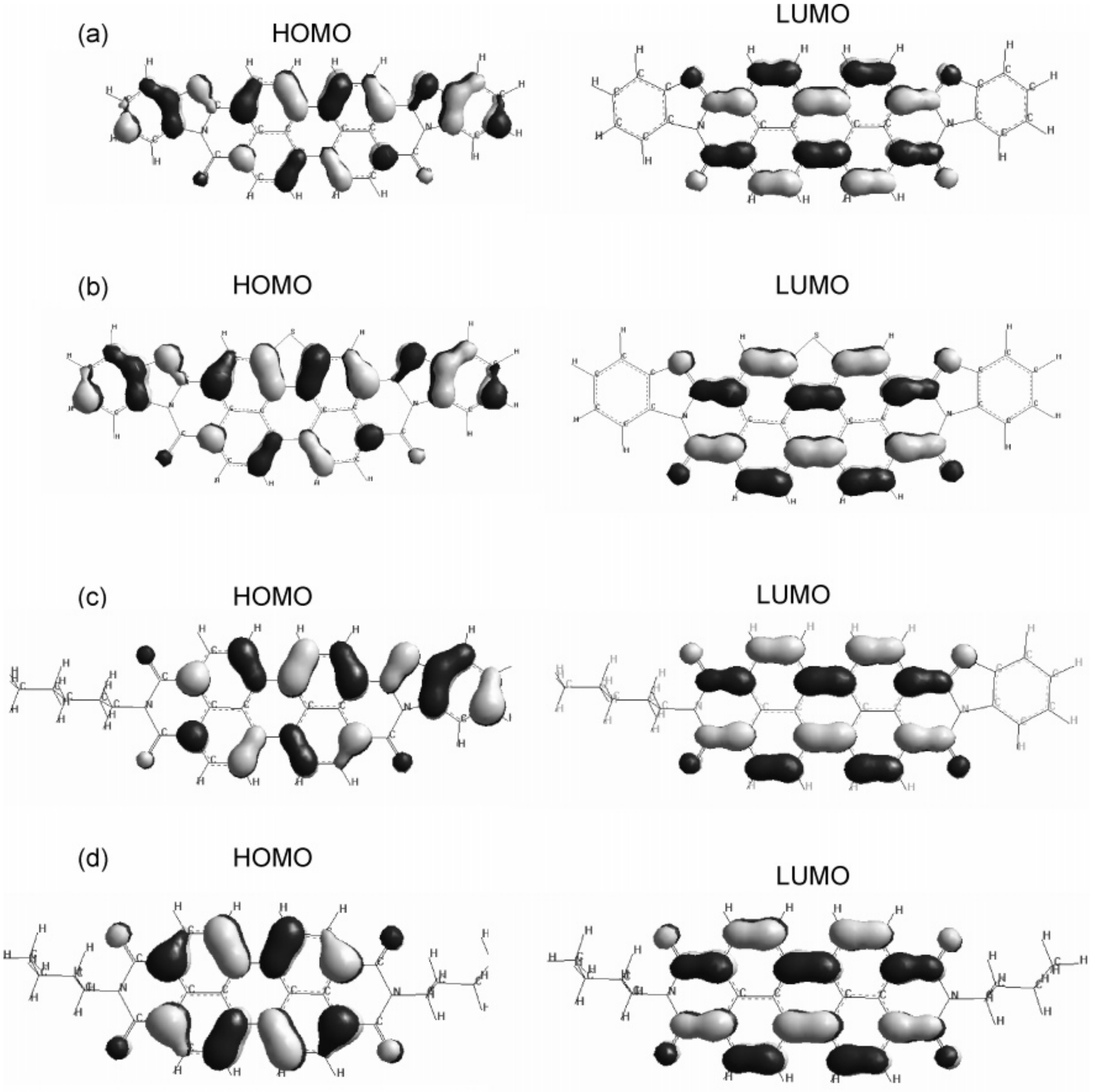

Figure 5. Representation of the molecular orbitals of HOMO and LUMO of AzoPTCD (a), Monothio BZP (b), PazoPTCD (c), and BuPTCB (d).

are mainly determined by the chromophore, with minimal effect from the lateral side groups. The differences observed in the nonlinear absorption spectra are essentially related to the resonance enhancement of the nonlinearity, starting at a different wavelength for each molecule, which is also shown in the SOS modeling.

Conclusions

The nonlinear absorption spectra of a perylene tetracarboxylic derivative (PTCD) family were determined by using the open aperture *Z*-scan technique. A sum-over-states (SOS) model was employed to fit the experimental data providing an accurate description of the nonlinearity resonant enhancement and the other features of nonlinear spectra. These compounds exhibit extremely large two-photon absorption (2PA) cross-sections in a wide spectral region, which make them strong candidates for photonics applications involving 2PA. The geometry optimization carried out with a semi-empirical method revealed that all the PTCDs have a central planar chromophore. Furthermore, the frontier molecular orbitals present similar features, indicating that nonlinear optical properties in PTCDs are mainly determined by the central portion of the molecule, with minimal effect from the lateral side groups. The differences observed in the nonlinear absorption spectra are essentially related to the resonance enhancement of the nonlinearity, provided by the favorable position of the energy levels.

Acknowledgment. Financial support from Fapesp (Fundação de Amparo a Pesquisa do Estado de São Paulo) and CNPq (Conselho Nacional de Desenvolvimento Científico) is gratefully acknowledged. We would like to thank Dr. J. Duff from XRCC for kindly providing us the samples, and also Dr. L. de Boni for helpful discussions.

References and Notes

(1) Graser, F.; Hadicke, E. *Liebigs Ann. Chem.* **1980**, 1994.

(2) Graser, F.; Hadicke, E. *Liebigs Ann. Chem.* **1984**, 483.

(3) Hadicke, E.; Graser, F. *Acta Crystallogr. Sect. C*: *Cryst. Struct. Commun.* **1986**, *42*, 195.

(4) Johnson, E.; Aroca, R.; Nagao, Y. *J. Phys. Chem.* **1991**, *95*, 8840.

(5) Sadrai, M.; Hadel, L.; Sauers, R. R.; Husain, S.; Kroghjespersen, K.; Westbrook, J. D.; Bird, G. R. *J. Phys. Chem.* **1992**, *96*, 7988.

(6) Ferrere, S.; Zaban, A.; Gregg, B. A. *J. Phys. Chem. B* **1997**, *101*, 4490.

(7) Oliveira, S. L.; Correa, D. S.; Misoguti, L.; Constantino, C. J. L.; Aroca, R. F.; Zilio, S. C.; Mendonca, C. R. *Adv. Mater.* **2005**, *17*, 1890.

(8) Kawata, S.; Sun, H. B.; Tanaka, T.; Takada, K. *Nature* **2001**, *412*, 697.

(9) Sun, H. B.; Kawata, S. Two-photon photopolymerization and 3D lithographic microfabrication. In *NMR−3D Analysis−Photopolymerization*; Springer−Verlag Berlin: Berlin, Germany, 2004; Vol. 170, p 169.

(10) Parthenopoulos, D. A.; Rentzepis, P. M. *J. Appl. Phys.* **1990**, *68*, 5814.

(11) Parthenopoulos, D. A.; Rentzepis, P. M. *Science* **1989**, *245*, 843.

(12) Bhawalkar, J. D.; He, G. S.; Prasad, P. N. *Rep. Prog. Phys.* **1996**, *59*, 1041.

(13) Dougherty, T. J.; Henderson, B. W.; Schwartz, S.; Winkelman, J. W.; Lipson, R. L. *Historical perspective. Photodynamic Therapy, Basic Principles and Clinical Application*; Henderson, B. W., Dougherty, T. J., Ed.; Marcel Dekker: New York, 1992; p 1.

(14) He, G. S.; Yuan, L. X.; Cui, Y. P.; Li, M.; Prasad, P. N. *J. Appl. Phys.* **1997**, *81*, 2529.

(15) Orr, B. J.; Ward, J. F. *Mol. Phys.* **1971**, *20*, 513.

(16) Kamada, K.; Ohta, K.; Yoichiro, I.; Kondo, K. *Chem. Phys. Lett.* **2003**, *372*, 386.

(17) Sheik-Bahae, M.; Said, A. A.; Van Stryland, E. W. *Opt. Lett.* **1989**, *14*, 955.

(18) Sheik-Bahae, M.; Said, A. A.; Wei, T. H.; Hagan, D. J.; Van Stryland, E. W. *IEEE J. Quantum Electron.* **1990**, *26*, 760.

(19) Dewar, M. J. S.; Zoebisch, E. G.; Healy, E. F.; Stewart, J. J. P. *J. Am. Chem. Soc.* **1985**, *107*, 3902.

(20) Ridley, J.; Zerner, M. *Theor. Chim. Acta* **1973**, *32*, 111.

(21) Franken, P. A.; Ward, J. F. *Rev. Mod. Phys.* **1963**, *35*, 23.

(22) Albota, M.; Beljonne, D.; Bredas, J. L.; Ehrlich, J. E.; Fu, J. Y.; Heikal, A. A.; Hess, S. E.; Kogej, T.; Levin, M. D.; Marder, S. R.; McCord-Maughon, D.; Perry, J. W.; Rockel, H.; Rumi, M.; Subramaniam, C.; Webb, W. W.; Wu, X. L.; Xu, C. *Science* **1998**, *281*, 1653.

(23) Kishi, R.; Nakano, M.; Yamada, S.; Kamada, K.; Ohta, K.; Nitta, T.; Yamaguchi, K. *Chem. Phys. Lett.* **2004**, *393*, 437.

(24) De Boni, L.; Misoguti, L.; Zilio, S. C.; Mendonca, C. R. *ChemPhysChem* **2005**, *6*, 1121.